Journal of Applied Electrochemistry **31**: 73–78, 2001.

Structural and electrochemical characteristics of $Li_{4/3}Ti_{5/3}O_4$ as an anode material for rechargeable lithium batteries

K. KANAMURA[1]*, T. UMEGAKI[1], H. NAITO[2], Z. TAKEHARA[2†] and T. YAO[3]
[1]*Department of Applied Chemistry, Graduate School of Engineering, Tokyo Metropolitan University, 1-1 Minami-Ohsawa, Hachiohji-shi, Tokyo 192-0397, Japan*
[2]*Department of Energy & Hydrocarbon Chemistry, Graduate School of Engineering, Kyoto University, Yoshida-honmachi, Sakyo-ku, Kyoto 606-8501, Japan*
[3]*Department of Fundamental Energy Science, Graduate School of Energy Science, Kyoto University, Yoshida-honmachi, Sakyo-ku, Kyoto 606-8501, Japan*
[†]*Present address: Department of Chemical Engineering, Faculty of Engineering, Kansai University, 3-35, Yamate-cho 3 chome, Suita, Osaka 564-8680, Japan*
*(*author for correspondence, fax: +81 426 77 2827, e-mail: kanamura-kiyoshi@c.metro-u.ac.jp)*

Received 16 September 1999; accepted in revised form 20 July 2000

Key words: anode, rechargeable lithium battery, Rietvled analysis, Ti oxides, UV–vis. spectroscopy

Abstract

$Li_{4/3}Ti_{5/3}O_4$ is a good anode material for rechargeable lithium batteries. This material exhibits characteristic properties, including very flat discharge and charge curves and an infinitesimal structural change during discharge and charge. In this study the structural behaviour was confirmed by the Rietveld analysis of X-ray diffraction patterns: *in situ* UV–visible spectroscopy of $Li_{4/3}Ti_{5/3}O_4$ during discharge was also performed to observe the electronic structure change induced by lithium insertion. The Rietveld analysis clearly showed that no structural change could be detected during the lithium insertion and extraction processes. The UV–vis. spectroscopy revealed that the insertion of lithium into $Li_{4/3}Ti_{5/3}O_4$ results in the formation of a new phase with the same lattice constant. These results indicate that the insertion and extraction of lithium into and from $Li_{4/3}Ti_{5/3}O_4$ proceed via two-phase reactions, while the lattice parameter is the same as that of $Li_{4/3}Ti_{5/3}O_4$ with lithium insertion.

1. Introduction

Various transition metal oxides have been investigated as cathode materials for rechargeable lithium batteries. Several researchers have also examined whether some transition metal oxides can be used as anode materials [1–9]. At the same time, some electronic devices with highly reliable rechargeable lithium batteries have been developed. These batteries are used to store electrical energy produced by solar energy or mechanical energy [10–12]. Rechargeable lithium batteries are intended for very long-term use, so that in devices containing such batteries, the batteries do not need changing during the lifetime of the devices. Therefore, high reliability of the rechargeable battery has to be achieved by using suitable materials for both cathode and anode. On the one hand, carbon has been used as anode material in rechargeable lithium batteries [13]. Its reliability is good enough for normal use, but is not good for use in the devices described above. On the other hand, transition metal oxides as insertion materials have shown highly reliable performance as cathodes [1–9], so that new oxide materials have been developed as anodes.

In particular, $Li_{4/3}Ti_{5/3}O_4$ has been investigated as an anode material for rechargeable lithium batteries, with a discharge potential of 1.5 V vs Li/Li^+ [14–18]. This compound has already been commercialized as a power accumulator for watches [10–12]. The most important characteristics of this compound as an anode material are not only its discharge and charge potential changes, but also the structural change that occurs during the discharge and charge cycles [14–18]. $Li_{4/3}Ti_{5/3}O_4$ has been prepared using various starting materials [16, 17]. Moreover, structural analysis of this compound during discharge and charge has been reported [17]. However, explanations of its unique electrochemical and structural behaviour have not yet been reported.

2. Experimental details

$Li_{4/3}Ti_{5/3}O_4$ has been prepared under various conditions. In this study, it was prepared by heating a mixture of Ti source (TiO_2 or Ti metal powder) and LiOH in a molar ratio of 5:4 at various temperatures under air atmosphere or oxygen atmosphere, in order to obtain well-defined crystalline $Li_{4/3}Ti_{5/3}O_4$. The crystal structures of prepared samples were analysed by X-ray diffraction. The electrochemical properties of these samples were investigated by cyclic voltammetry. For this measurement, propylene carbonate containing 1.0 mol dm^{-3} $LiClO_4$ was used as the solvent. Lithium metal foil was used as the reference and counter electrodes. The sweep rate was 10 mV min^{-1}. In addition, a discharge and charge cycle test was also conducted under galvanostatic conditions in order to examine the rechargeability of $Li_{4/3}Ti_{5/3}O_4$. The discharge and charge currents were 0.5 mA cm^{-2} and the electrolyte solution was the same as that used for the cyclic voltammetry. The structural change of $Li_{4/3}Ti_{5/3}O_4$ during the discharge and charge cycle was also investigated using X-ray diffraction. The refinement of the crystal structure of $Li_{4/3+x}Ti_{5/3}O_4$ ($x = 0$, 0.5 after the first discharge, 1.0 after the first discharge, 0.5 after the first charge, 0 after the first charge) was performed using the Rietveld analysis for the X-ray diffraction patterns [19]. A Cu or Mo K_α line was used as the X-ray source. A diffractometer with a graphite monochrometer was used to collect the X-ray diffraction data. The Rietveld analysis was conducted using the RIVEC program in Kyoto University. A vector computer was used to calculate the simulated X-ray diffraction pattern. The calculation was continued until the R_{wp} value decreased to less than 15%.

The electronic state of $Li_{4/3}Ti_{5/3}O_4$ has been reported earlier [20, 21]. The electronic state should be changed during the course of the insertion or extraction of lithium. This change leads to a colour change in the $Li_{4/3}Ti_{5/3}O_4$. This colour change should be related to the mechanisms of the insertion and extraction. In this study, *in situ* UV–vis. spectroscopy was employed to observe the colour change. Figure 1 shows an *in situ* electrochemical UV–vis. spectroscopic cell with SiO_2 window. Lithium foil was used as the counter electrode. Propylene carbonate with 1.0 mol dm^{-3} $LiClO_4$ was used as the electrolyte. The cell was discharged under galvanostatic conditions at 0.5 mA cm^{-2}, and the UV–vis. spectra were collected simultaneously at several discharge stages.

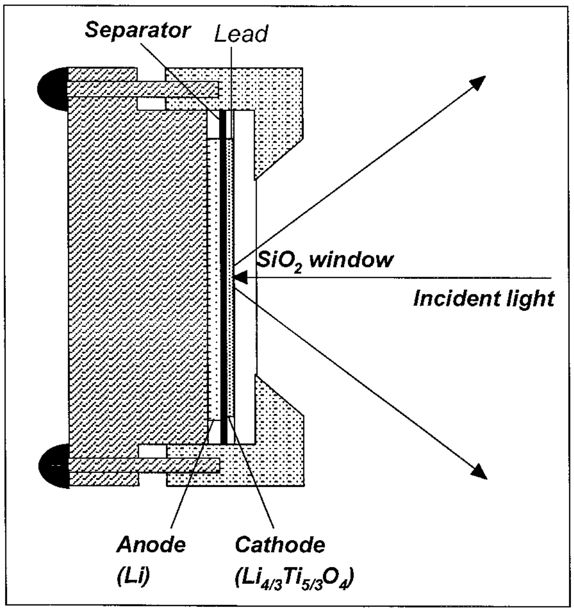

Fig. 1. Schematic illustration of *in situ* electrochemical UV–vis. spectroscopy for a rechargeable lithium battery with $Li_{4/3}Ti_{5/3}O_4$ and lithium metal, electrolyte: propylene carbonate containing 1.0 mol dm^{-3} $LiClO_4$, current collector: Ti mesh and Ni mesh, window: SiO_2.

3. Results and discussion

3.1. *Rietveld analysis of discharge and charge process of* $Li_{4/3}Ti_{5/3}O_4$

Figure 2 shows X-ray diffraction patterns of reaction products prepared under various conditions. The samples (a)–(f) were prepared from Ti metal powder and LiOH. Most of the main peaks are attributable to spinel structures, but several peaks are attributable to other Ti oxides. This means that the reaction products do not consist of a single $Li_{4/3}Ti_{5/3}O_4$ spinel phase. Three samples (g)–(i) were prepared from TiO_2 and LiOH. The patterns of these samples indicated a cubic spinel structure. However, the peak intensities of the three samples varied. The most ideal cubic spinel structure was obtained by heating a mixture of LiOH and TiO_2 at 800 °C under air atmosphere. Figure 3 shows the X-ray diffraction patterns of $Li_{4/3}Ti_{5/3}O_4$ obtained under the above conditions, and of that simulated by the Rietveld analysis. The observed pattern was in good agreement with the simulated one. This means that the product has a cubic spinel structure with an $Fd\bar{3}m$ space group. In this calculation, the 16d sites in the spinel structure were occupied by both Ti^{4+} ions and Li^+ ions with molar ratio of 5:1, so that the reaction product can be described as $[Li]_{8a}[Li_{1/3}Ti_{5/3}]_{16d}[O_4]_{32e}$. The lattice parameter of this oxide was determined to be 8.356 66(1) and its oxygen positional parameter was estimated to be 0.387 0(2).

Some groups studied the usefulness of $Li_{4/3}Ti_{5/3}O_4$ as an insertion electrode [14–18], and the findings suggested two interesting behaviours. The first was a small electrode potential change as x in $Li_{4/3+x}Ti_{5/3}O_4$ changed. The second was the lack of a detectable lattice constant change during lithium insertion and extraction. To confirm the lack of a detectable structural change of $Li_{4/3}Ti_{5/3}O_4$, Rietveld analysis was conducted for the X-ray diffraction patterns of $Li_{4/3}Ti_{5/3}O_4$ before and after the electrochemical insertion or extraction of lithium. The prepared $Li_{4/3}Ti_{5/3}O_4$ was galvanostatically discharged or charged at 0.2 mA cm^{-2} and the structure was then analysed by X-ray diffraction.

Figure 4 shows the X-ray diffraction patterns at $x = 0$, $x = 0.5$, $x = 1.0$ after discharge, and $x = 0.5$ after charge in $Li_{4/3+x}Ti_{5/3}O_4$. The precise lattice parameters and oxygen parameters for various discharge

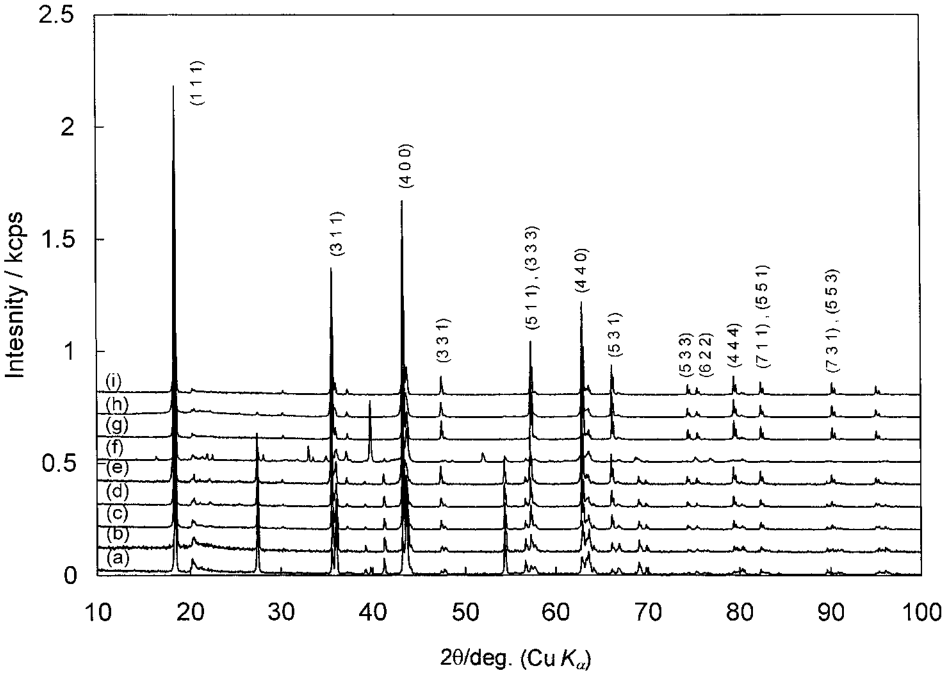

Fig. 2. X-ray diffraction patterns of products prepared under various conditions: (a) Ti + LiOH, 700 °C, air; (b) Ti + LiOH, 750 °C, air; (c) Ti + LiOH, 800 °C, air; (d) Ti + LiOH, 850 °C, air; (e) Ti + LiOH, 900 °C, air; (f) Ti + LiOH, 800 °C, argon; (g) TiO_2 + LiOH, 800 °C, air; (h) Li_2CO_3 + TiO_2, 900 °C, O_2/CO_2 (1:1); (i) TiO_2 + LiOH, 800 °C, argon.

or charge stages were determined by Rietveld analysis of these patterns. All X-ray diffraction patterns were well simulated by our Rietveld analysis. All R_{wp} values were less than 12%, indicating that the obtained lattice parameters and oxygen parameters were very precise. The lattice parameters and oxygen parameters are plotted in Figure 5, which clearly shows that neither lattice nor oxygen positional parameters change significantly during lithium insertion and extraction. For example, the expansion of the unit volume was less than 0.3% before and after the complete discharge or charge. In general, the peak shift in a lower 2θ angle region is smaller than that in a higher one. In order to check the lattice expansion of $Li_{4/3}Ti_{5/3}O_4$, the peak shift in a

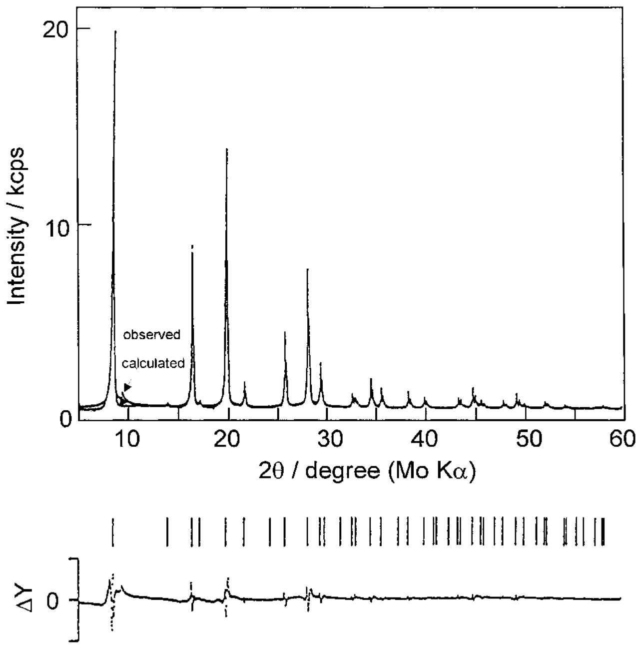

Fig. 3. X-ray diffraction pattern for compound prepared under the conditions of TiO_2 + LiOH, 800 °C, and air, and the pattern simulated by Rietveld analysis.

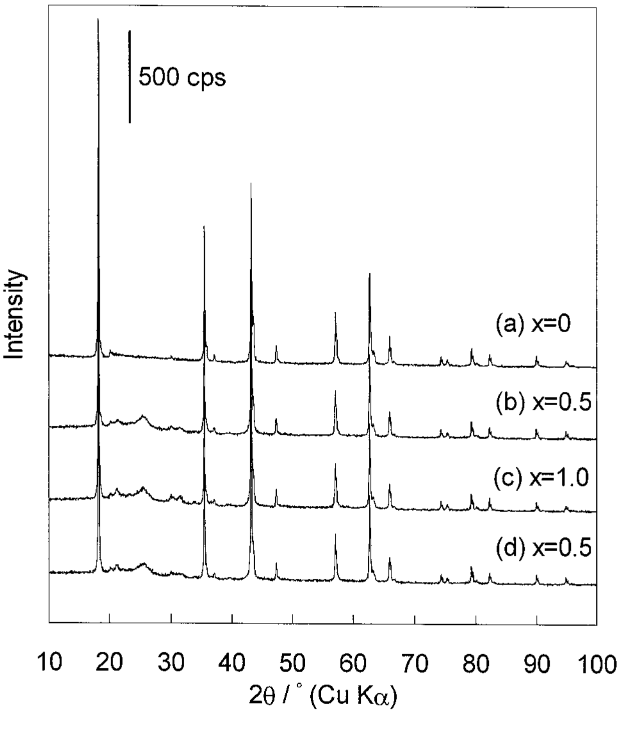

Fig. 4. X-ray diffraction patterns for $Li_{4/3+x}Ti_{5/3}O_4$ prepared in this study (Figure 2(g)). (a) $x = 0$, (b) $x = 0.5$ after the discharge, (c) $x = 1.0$ after the discharge, and (d) $x = 0.5$ after the charge.

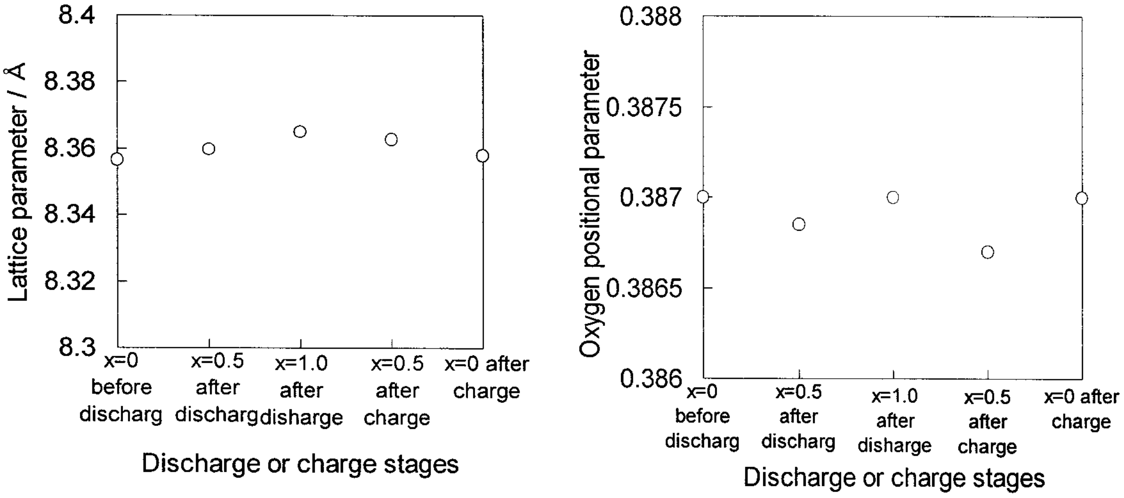

Fig. 5. Lattice parameter and oxygen positional parameter changes during discharge and charge obtained by Rietveld analysis of the X-ray diffraction patterns of $Li_{4/3+x}Ti_{5/3}O_4$ prepared in this study (Figure 2(g)). (a) $x = 0$, (b) $x = 0.5$ after the discharge, (c) $x = 1.0$ after the discharge, and (d) $x = 0.5$ after the charge.

higher angle region was investigated. Figure 6 shows the peak in the 2θ region from 70° to 80°; no peak shift was observed, even in this higher 2θ region. These results clearly indicate that the original crystal structure is essentially maintained during insertion and extraction of lithium. This behavior is not usually observed when transition metal oxides are used as cathode or anode materials in rechargeable lithium batteries.

3.2. *Electrochemical characteristics of $Li_{4/3}Ti_{5/3}O_4$*

Figure 7(a) and (b) show the discharge and charge curves of $Li_{4/3}Ti_{5/3}O_4$ and the discharge capacity change during these cycles, respectively. The discharge and charge curves were very flat, as discussed above. This electrode potential change corresponds to the free energy change of

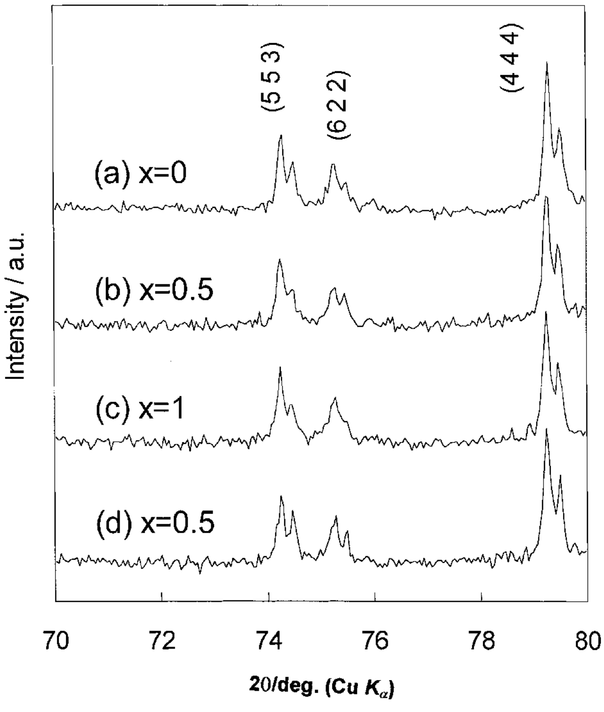

Fig. 6. X-ray diffraction patterns on an expanded scale for $Li_{4/3+x}Ti_{5/3}O_4$ prepared in this study (Figure 2(g)). (a) $x = 0$, (b) $x = 0.5$ after the discharge, (c) $x = 1.0$ after the discharge, and (d) $x = 0.5$ after the charge.

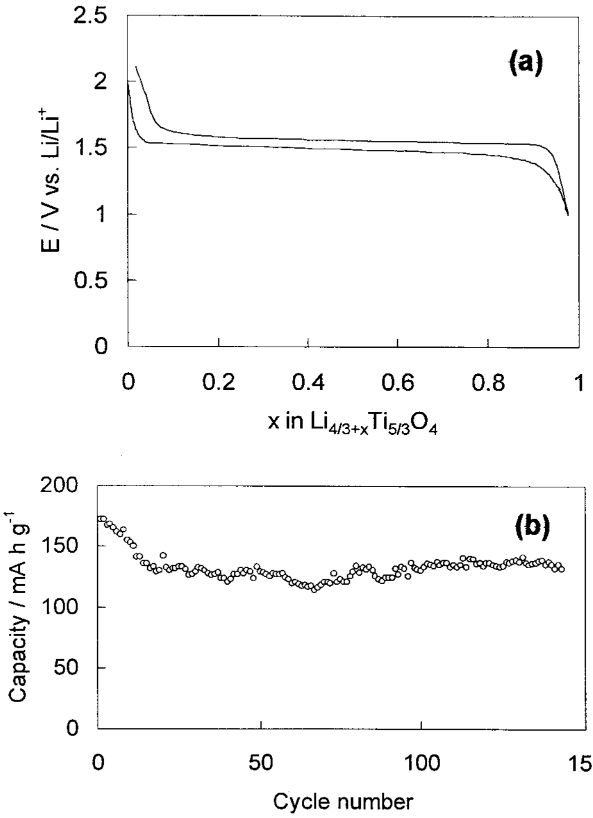

Fig. 7. Discharge and charge curves of $Li_{4/3}Ti_{5/3}O_4$ prepared in this study (Figure 2(g)) at 0.5 mA cm^{-2} in propylene carbonate containing 1.0 mol dm^{-3} $LiClO_4$, and discharge capacity change during discharge and charge cycles under the same conditions.

$Li_{4/3}Ti_{5/3}O_4$ as x changes in $Li_{4/3+x}Ti_{5/3}O_4$. Therefore, it can be said that the free energy of $Li_{4/3+x}Ti_{5/3}O_4$ does not change depending on the amount of lithium inserted into $Li_{4/3}Ti_{5/3}O_4$. If a homogeneous phase of $Li_{4/3+x}Ti_{5/3}O_4$ were formed by the insertion of lithium, the electrode potential change should not be flat and, correspondingly, the free energy should change. The electrode potential change strongly indicates that the electrochemical reaction of $Li_{4/3}Ti_{5/3}O_4$ proceeds via a two-phase reaction. However, the X-ray diffraction pattern of $Li_{4/3}Ti_{5/3}O_4$ did not show the formation of any new phases at all. These results are inconsistent with each other.

The discharge capacity change in Figure 7(b) was very stable during the different cycles. A similar result is sometimes obtained when the structural change of a transition metal oxide during discharge and charge cycles is enough small to permit maintenance of the original structure. This discharge capacity change is in good agreement with the X-ray diffraction data.

Figure 8 shows the cyclic voltammogram of $Li_{4/3}Ti_{5/3}O_4$ at 10 mV min^{-1} in propylene carbonate containing 1.0 mol dm^{-3} $LiClO_4$. Very sharp anodic and cathodic peaks were observed at around 1.5 V vs Li/Li^+. The electrode potential of the cathodic peak was different from that of the anodic peak. These characteristics of the redox peak showed that a two-phase reaction can provide an explanation of the electrode kinetics of $Li_{4/3}Ti_{5/3}O_4$. From both electrochemical experiments, it can be seen that the electrode reaction can be explained by a two-phase reaction in spite of the lack of observation of any new phases from the X-ray diffraction patterns.

3.3. In situ *UV–vis. spectroscopy of* $Li_{4/3}Ti_{5/3}O_4$

If the insertion of lithium into $Li_{4/3}Ti_{5/3}O_4$ proceeds via a two-phase reaction, one new phase can be considered to be $Li_{7/3}Ti_{5/3}O_4$, based on the discharge capacity. However, no new phases were observed in our X-ray diffraction patterns. This may indicate that $Li_{7/3}Ti_{5/3}O_4$ has almost the same lattice parameters as those of $Li_{4/3}Ti_{5/3}O_4$ if a two-phase reaction indeed occurs. However, explaining the flat potential by invoking a two-phase reaction is questionable, because there is no driving force for a phase separation when crystal structures of two phases have the same lattice constant. No evidence of a homogeneous or two-phase reaction was obtained from the X-ray diffraction patterns of $Li_{4/3}Ti_{5/3}O_4$. In this study, a further analysis was performed using UV–vis. spectroscopy, because the colour of $Li_{4/3}Ti_{5/3}O_4$ changed from white to dark blue upon lithium insertion, indicating that the electronic state changes with the insertion of lithium. The band structure of $Li_{4/3}Ti_{5/3}O_4$ has been reported [20, 21]. This material is originally an insulator, because all Ti ions are in a 4+ valence state. Upon insertion of lithium, the valence state of the Ti ions is changed from 4+ to 3+, leading to a change in the electronic state of $Li_{4/3}Ti_{5/3}O_4$.

Figure 9 shows the UV–vis. spectra for $Li_{4/3}Ti_{5/3}O_4$ at various discharge stages. Before discharge, there was no absorption at wavelengths ranging from 300 to 2000 nm, corresponding to the white colour of $Li_{4/3}Ti_{5/3}O_4$. After insertion of lithium at $x = 0.02$ in $Li_{4/3+x}Ti_{5/3}O_4$, a strong, broad absorption peak was observed, which corresponded to the dark blue colour. This result directly indicates that the electronic structure of $Li_{4/3}Ti_{5/3}O_4$ changes upon lithium insertion

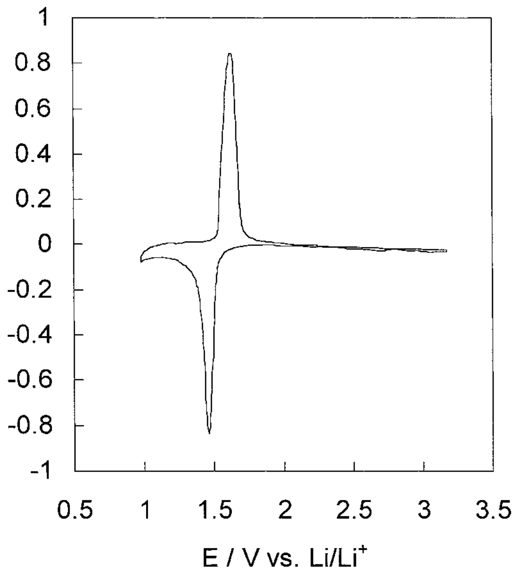

Fig. 8. Cyclic voltammogram of $Li_{4/3}Ti_{5/3}O_4$ prepared in this study (Figure 2(g)) in propylene carbonate containing 1.0 mol dm^{-3} $LiClO_4$ at 10 mV min^{-1}.

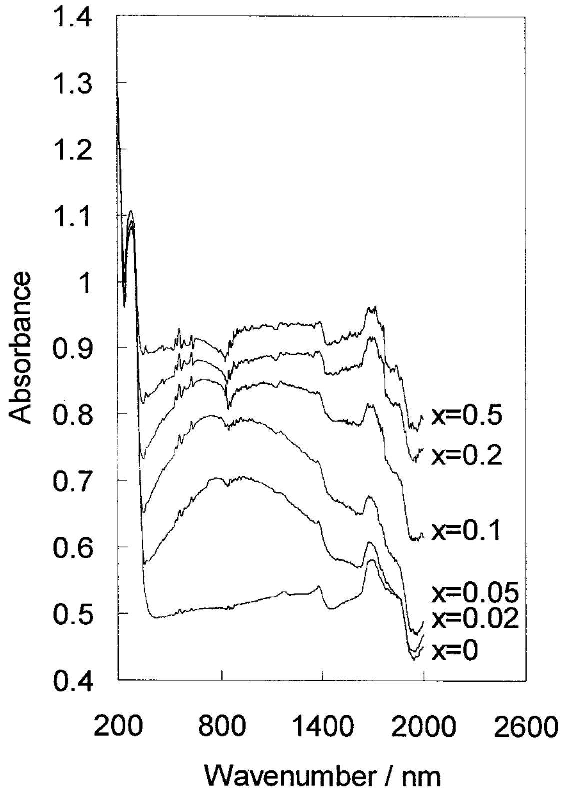

Fig. 9. In situ UV–vis. spectra of $Li_{4/3+x}Ti_{5/3}O_4$ prepared in this study (Figure 2(g)), $x = 0$, $x = 0.02$, $x = 0.05$, $x = 0.1$, $x = 0.2$ and $x = 0.5$.

associated with the reduction of Ti^{4+} to Ti^{3+}. The transition of an electron takes place when the light has an energy corresponding to the band gap of $Li_{4/3}Ti_{5/3}O_4$ (3.0 eV). However, this band gap is too large to permit absorption of visible light. The lack of absorption at wavelengths ranging from 300 to 2000 nm is in good agreement with the band structure. After the insertion of lithium at $x = 0.02$, electrons were generated in the conduction band of $Li_{4/3}Ti_{5/3}O_4$ corresponding to a reduction of Ti^{4+} to Ti^{3+}, producing a new electron transition from the conduction band to higher energy levels. Probably, the blue colour corresponds to this new electron transition. The energy level generated by the insertion of lithium into $Li_{4/3}Ti_{5/3}O_4$ depends on the number of electrons inserted when there is a homogeneous insertion of lithium. On the one hand, this means that the shape of the absorption spectrum (the peak of the absorption) changes depending on the amount of lithium inserted. On the other hand, when a two-phase reaction takes place during lithium insertion, the shape of the absorption spectrum (the peak of the absorption) does not change with the amount of lithium inserted into $Li_{4/3}Ti_{5/3}O_4$. In other words, only the intensity of the absorption spectrum is changed by the lithium insertion. In the present study, the shape of the absorption spectrum was not changed by the lithium insertion (Figure 9). In the region $x > 0.5$, uniform absorption was observed at wavelengths ranging from 300 to 1800 nm. This may have been caused by the high electron conduction of the $Li_{4/3+x}Ti_{5/3}O_4$ ($x > 0.5$) electrode. Therefore, at all values of x, the peak wavelength in the absorption spectrum was not changed by the lithium insertion, indicating that the electrochemical insertion of lithium into $Li_{4/3}Ti_{5/3}O_4$ takes place in a two-phase reaction. $Li_{4/3}Ti_{5/3}O_4$ and $Li_{7/3}Ti_{5/3}O_4$ coexist during the lithium insertion, and both crystals have almost the same lattice constant.

4. Conclusions

Rietveld analysis for the X-ray diffraction patterns at various discharge and charge stages indicated the lack of a detectable structural change of $Li_{4/3}Ti_{5/3}O_4$. This result was in good agreement with previous results reported by several groups. Moreover, the *in situ* UV–vis. spectra clearly showed the possibility that lithium insertion into $Li_{4/3}Ti_{5/3}O_4$ is associated with the formation of a new phase. These results indicate that the new phase has the same structure as the original $Li_{4/3}Ti_{5/3}O_4$, but a different Li content.

References

1. J.M. Tarascon and D. Guyomard, *Electrochim. Acta* **38** (1993) 1221.
2. T. Ohzuku, M. Kitagawa and T. Hirai, *J. Electrochem. Soc.* **137** (1990) 769.
3. J.R. Dahn, U. von Sacken, M.W. Juzkow and H. Al-Janaby, *J. Electrochem. Soc.* **138** (1991) 2207.
4. J.N. Reimers and J.R. Dahn, *J. Electrochem. Soc.* **139** (1992) 2091.
5. E. Plichta, S. Slane, M. Uchiyama, M. Salomon, D. Chua, W.B. Ebner and H.W. Lin, *J. Electrochem. Soc.* **136** (1989) 1865.
6. E. Rossen, J.N. Reimer and J.R. Dahn, *Solid State Ionics* **62** (1993) 53.
7. M.M. Thackeray, P.J. Johnson, L.A. de Picciotto, P.G. Bruce and J.B. Goodenough, *Mater. Res. Bull.* **19** (1984) 179.
8. M.M. Thackeray, W.I.F. David, P.G. Bruce and J.B. Goodenough, *Mater. Res. Bull.* **18** (1983) 461.
9. N. Furukawa, T. Nohma, K. Teraji, I. Nakane and T. Saito, *Denki Kagaku* **57** (1989) 533.
10. N. Koshiba, K. Takata, M. Nakanishi, E. Asaka and Z. Takehara, *Denki Kagaku* **62** (1994) 870.
11. N. Koshiba, K. Takata, M. Nakanishi, E. Asaka and Z. Takehara, *Denki Kagaku* **62** (1994) 593.
12. N. Koshiba, K. Takata, M. Nakanishi, K. Chikayama and Z. Takehara, *Denki Kagaku* **62** (1994) 970.
13. K. Kanamura, *Denki Kagaku* **65** (1997) 722.
14. T. Ohzuku, A. Ueda, N. Yamamoto and Y. Iwakoshi, *J. Power Sources* **54** (1995) 9.
15. D.W. Murphy, R.J. Cava, S.M. Zahurak and A. Santora, *Solid State Ionics* **9–10** (1983) 413.
16. K.M. Colbow, J.R. Dahn and R.R. Haering, *J. Power Sources* **26** (1989) 397.
17. T. Ohzuku, A. Ueda and N. Yamamoto, *J. Electrochem. Soc.* **142** (1995) 1431.
18. M.M. Thackeray, *J. Electrochem. Soc.* **142** (1995) 2558.
19. K. Kanamura, H. Naito, T. Yao and Z. Takehara, *J. Mater. Chem.* **6** (1996) 33.
20. M.R. Harrison, P.P. Edwards and J.B. Goodenough, *Phil. Mag. B* **52** (1985) 679.
21. P.G. Dickens, A.C. Halliwell, D.J. Murphy and M.S. Whittingham, *Trans. Faraday Soc.* **67** (1971) 794.
22. S.J. Martin, M. O'Keeffe and D.E. Partin, *J. Solid State Chem.* **113** (1994) 413.
23. R. Horyn, M. Wolcyrz and A. Wojakowski, *J. Solid State Chem.* **116** (1995) 68.